INSTITUT DE FRANCE
Académie des sciences

Comptes Rendus

Mécanique

M. H. Tchiekre, A. D. V. Brou and J. K. Adou

Deterministic optimization techniques to calibrate parameters in a wildland fire propagation model

Volume 348, issue 8-9 (2020), p. 759-768

Published online: 14 December 2020

https://doi.org/10.5802/crmeca.58

Les Comptes Rendus. Mécanique *sont membres du Centre Mersenne pour l'édition scientifique ouverte*
www.centre-mersenne.org
e-ISSN : 1873-7234

Comptes Rendus
Mécanique
2020, 348, nº 8-9, p. 759-768
https://doi.org/10.5802/crmeca.58

Short paper / *Note*

Deterministic optimization techniques to calibrate parameters in a wildland fire propagation model

M. H. Tchiekre[a], **A. D. V. Brou**[*, b] **and J. K. Adou**[a]

[a] Université FHB d'Abidjan, UFR Math. Info., 22 BP 582 Abidjan 22, Côte d'Ivoire

[b] Université JLG de Daloa, UFR Environnement, BP 150 Daloa, Côte d'Ivoire

E-mails: mhtchiekre@gmail.com (M. H. Tchiekre), brou.akahoua@ujlg.edu.ci (A. D. V. Brou), jkadou@hotmail.com (J. K. Adou)

Abstract. To fight against forest fires, simple and improved models are more searched out due to the fact they are more easily understandable by the users. This actual model is part of the fire propagation models within a network. It is simple and easy to implement. However, it depends on several parameters that are difficult to measure or estimate precisely beforehand. The prediction by this model is therefore insufficient. A deterministic optimization method is introduced to calibrate its parameters. The optimized model was tested on several laboratory experiments and on two large-scale experimental fires. The comparison of the model results with those of the experiment shows a very significant improvement in its prediction with the optimal parameters.

Résumé. Dans la lutte contre les feux de forêt, les modèles simples et améliorés sont plus recherchés car plus aisément compréhensibles par les utilisateurs. Le présent modèle fait partie des modèles de propagation de feu à l'intérieur d'un réseau. Il est simple et facile à mettre en œuvre. Cependant, il dépend de plusieurs paramètres difficiles à mesurer ou à estimer avec précision au préalable. La prédiction par ce modèle est de ce fait insuffisante. Par conséquent, une méthode déterministe d'optimisation est introduite pour calibrer ses paramètres. Le modèle optimisé a été testé sur plusieurs feux de laboratoires et sur deux feux expérimentaux à grande échelle. La comparaison des résultats du modèle avec ceux de l'expérience montre une amélioration très significative de sa prédiction avec les paramètres optimaux.

Keywords. Optimization method, Calibration parameter, Rate of spread, Fire propagation, Firefighting, Fire behavior, Modeling.

Manuscript received 25th July 2020, revised 2nd November 2020, accepted 17th November 2020.

* Corresponding author.

1. Introduction

Forest fires are complex phenomena, and the difficulties of their modeling comes on the one hand from the lack of knowledge on the detail of certain processes involved in the physics of these phenomena and on the other hand the large number of data required by these models.

Several fire propagation models are developed in the literature. Among them, we have the so-called deterministic models [1–3] based on the physics of the phenomenon. Such models are detailed, but require a lot of resources and are therefore difficult to implement. We also have the so-called semi-physical models [4–7] which are less detailed than the first ones, but more operational in the fight against fires propagation, because they are faster in implementation [8].

Most of these models depend on large number of parameters, and some of them are difficult to assess. The uncertainties related to the values of these parameters can deteriorate the quality of prediction of these models. Hence, there is the need to make a good calibration of model parameters.

Several methods to assess the parameters of fire propagation models exist in the literature. D. Ascoli *et al.* [9] used the genetic algorithm to calibrate the fuel input data in the Rothermel model. The fuel data in this model comes from correlations based on vegetation in North America and is therefore not suitable for other regions. The execution time remains the constraint for this method.

T. Artés *et al.* [10] have developed a calibration method based on the genetic algorithm and have a shorter execution time. However, the complex implementation and computational resource requirements are the weaknesses of this method.

In this paper, we present a parametric optimization method, based on the minimization of a "cost" function coming from the difference between the real pattern of fires and that predicted by the model.

2. Model

The present model is built from a two-dimensional regular network of equal-size cells (Figure 1). It is assumed that each combustible cell j has a cylindrical shape with a height H_j and a diameter diam_j. A combustible cell j is said to be healthy when its temperature T_j is equal to the ambient temperature T_∞. The energy absorbed by the combustible cell when it is exposed to the fire front is used to raise the temperature of wet fine fuel elements to the boiling temperature of water, 373 K, evaporate the moisture, and raise the temperature of dry fine fuel elements to the ignition temperature T_{ign}. The combustible cell then continues to burn with a flame, while transferring heat to the neighboring cells by means of convection and radiation. In the solid flame model, the visible flame is regarded as a uniformly radiating solid body with a cylindrical shape and with thermal radiation emitted from its surface.

The total energy q_j absorbed by cell j is used on the one hand to raise the temperature of fine fuel elements and on the other hand to evaporate moisture at the boiling temperature of water.

$$q_j = \begin{cases} \rho_j C_{pj} \phi_j \dfrac{\mathrm{d}T_j}{\mathrm{d}t}, & \text{for } T_j \neq 373 \text{ K} \\ -\rho_j h_{\mathrm{vap}} \phi_j \dfrac{\mathrm{d}W_j}{\mathrm{d}t}, & \text{for } T_j = 373 \text{ K}, \end{cases} \tag{1}$$

where T_j and W_j are respectively the mean temperature and the mass fraction of water of cell j, ρ_j is the fuel particle density, C_{pj} is the specific heat capacity, h_{vap} is the specific enthalpy change of water to vapor at 373 K, and ϕ_j is the packing ratio.

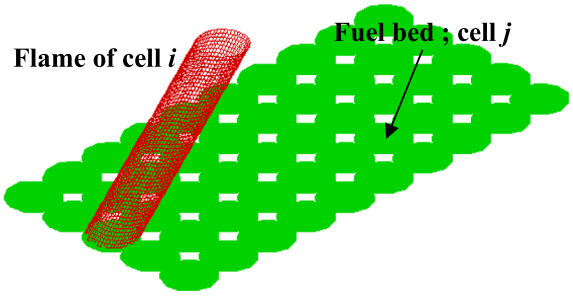

Figure 1. Solid flame model and schematic of the network showing a burning cell i and a healthy cell j.

Let N_j be the number of burning cells that interact with cell j, we have

$$q_j = \sum_{i=1}^{N_j} q_{ij}, \tag{2}$$

where q_{ij} is the total heat flux emitted from the burning cell i which is received by cell j. It is the sum of all possible heat transfer mechanisms: radiation on the top surface of cell j, internal radiation from the ember zone, convection on the top surface of cell j, internal convection inside the fuel bed, radiation loss to the ambient on the top surface of cell j, and is given by the following relation.

$$\begin{aligned} q_{ij} = & \underbrace{\frac{a_{\mathrm{fb}}\varepsilon_{\mathrm{fl}}\sigma T_{\mathrm{fl}}^4}{H_j}F_{ij}}_{\substack{\text{surface}\\ \text{radiation}}} + \underbrace{0.25A_{\mathrm{fb}}\varepsilon_b\sigma T_b^4\exp(-0.25A_{\mathrm{fb}}d_{ij})}_{\substack{\text{internal}\\ \text{radiation}}} \\ & + \underbrace{\frac{0.565k_{\mathrm{fl}}Re_{d_{ij}}^{1/2}Pr^{1/2}}{d_{ij}H_j}(T_{\mathrm{fl}}-T_j)\exp(-0.3d_{ij}/L_{\mathrm{fl}})\beta_{ij}}_{\substack{\text{surface}\\ \text{convection}}} \\ & + \underbrace{\frac{0.911A_{\mathrm{fb}}k_bRe_D^{0.385}Pr^{1/3}}{\mathrm{diam}_j}(T_b-T_j)\exp(-0.25A_{\mathrm{fb}}d_{ij})\beta_{ij}}_{\substack{\text{internal}\\ \text{convection}}} - \underbrace{\frac{\varepsilon_{\mathrm{fb}}\sigma(T_j^4-T_\infty^4)}{H_j}}_{\substack{\text{radiative}\\ \text{loss}}}. \end{aligned} \tag{3}$$

The flame emissivity $\varepsilon_{\mathrm{fl}} = 1-\exp(-0.6L_{\mathrm{fl}})$, where L_{fl} is the flame length, a_{fb} is the fuel bed absorptivity, and σ ($= 5.67\times10^{-8}$ W/m^2/K) is the Stefan–Boltzmann constant. F_{ij} is the view factor, ε_b is the ember emissivity, and T_b its temperature. A_{fb} is the total fuel particle surface area per fuel bed volume. $\varepsilon_{\mathrm{fb}}$ is the fuel bed emissivity and d_{ij} is the distance between cell i and cell j. Pr is the Prandtl number and $Re_{d_{ij}}$ is the Reynolds number based on the length scale d_{ij}. k_{fl} and T_{fl} are respectively the thermal conductivity and the flame temperature. Re_{D_j} is the Reynolds number based on the branch diameter diam_j as length scale. β_{ij} is a coefficient which is equal to unity when the straight line connecting cells i and j is aligned with the wind direction, and zero otherwise.

The reader who is interested by the model will find more details in Adou *et al.* [11].

The model allows to describe the rate of spread and the fire contour through the evolution of temperature T_j of cells j given by (1). Taking relation (2) into account, this equation can, for $T_j \neq 373$ K, be rewritten as

$$\begin{cases} \dfrac{\mathrm{d}T_j}{\mathrm{d}t} = \displaystyle\sum_{i=1}^{N_j} S_{ij}(T_j(t)) \\ T_j(0) = T_\infty, \end{cases} \tag{4}$$

where

$$S_{ij} = \frac{1}{\rho_j C_{pj} \phi_j} q_{ij}, \tag{5}$$

with q_{ij} is given by (3).

3. Description of the parametric optimization method

Scrutinizing the expression of S_{ij} in (5), we notice that it depends not only on the temperature T_j, but also on a set of parameters. We can classify these parameters into two types. We have on the one hand the parameters whose values are assumed to be known with relative exactness which we will call input data, and on the other hand those which are known with uncertainty. Let θ be the vector whose components are the parameters of the second type. For our model, we have

$$\theta = (a_{\mathrm{fb}}, T_{\mathrm{fl}}, \varepsilon_b, \varepsilon_{\mathrm{fb}}, k_{\mathrm{fl}}, k_b, T_b)^T. \tag{6}$$

According to several authors in the literature (see for example [12–15]), the components θ_l ($l = 1, \ldots, 7$) generally vary in the following intervals.

$$\begin{cases} a_{\mathrm{fb}} \in [0.3; 1]; T_{\mathrm{fl}} \in [700; 1200]; \varepsilon_b \in [0.1; 1]; \varepsilon_{\mathrm{fb}} \in [0.1; 1] \\ k_{\mathrm{fl}} \in [0.0371; 0.225]; k_b \in [0.0205; 0.105]; T_b \in [500; 700]. \end{cases} \tag{7}$$

We can therefore define a so-called physically admissible set $\Omega \subset \mathbb{R}^7$ in which θ varies. This set is the Cartesian product of the above intervals namely,

$$\Omega = [0.3; 1] \times [700; 1200] \times [0.1; 1] \times [0.1; 1] \times [0.0371; 0.225] \times [0.0205; 0.105] \times [500; 700]. \tag{8}$$

Finally, the term S_{ij} in (5) can be rewritten using the components of θ as follows:

$$S_{ij}(\theta, T_j) = \underbrace{A_{ij}\theta_1\theta_2^4}_{\substack{\text{surface} \\ \text{radiation}}} + \underbrace{B_{ij}\theta_3\theta_7^4}_{\substack{\text{internal} \\ \text{radiation}}} + \underbrace{D_{ij}\theta_5(\theta_2 - T_j)}_{\substack{\text{surface} \\ \text{convection}}} + \underbrace{E_{ij}\theta_6(\theta_7 - T_j)}_{\substack{\text{internal} \\ \text{convection}}} - \underbrace{C_{ij}\theta_4(T_j^4 - T_\infty^4)}_{\substack{\text{radiative} \\ \text{loss}}}, \tag{9}$$

where

$$\begin{cases} A_{ij} = \dfrac{\varepsilon_{\mathrm{fl}}\sigma}{\rho_j C_{pj}\phi_j H_j} F_{ij}; \quad B_{ij} = \dfrac{0.25 A_{\mathrm{fb}}\sigma \exp(-0.25 A_{\mathrm{fb}} d_{ij})}{\rho_j C_{pj}\phi_j}; \quad C_{ij} = \dfrac{\sigma}{\rho_j C_{pj}\phi_j H_j} \\ D_{ij} = \dfrac{0.565 Re_{d_{ij}}^{\frac{1}{2}} Pr^{\frac{1}{2}}}{\rho_j C_{pj}\phi_j d_{ij} H_j} \exp\left(-\dfrac{0.3 d_{ij}}{L_{\mathrm{fl}}}\right)\beta_{ij}; \quad E_{ij} = \dfrac{0.911 A_{\mathrm{fb}} Re_D^{0.385} Pr^{1/3}}{\rho_j C_{pj}\phi_j \mathrm{diam}_j} \exp(-0.25 A_{\mathrm{fb}} d_{ij})\beta_{ij}. \end{cases} \tag{10}$$

The system (4) giving the evolution of temperature T_j can be rewritten in the following form.

$$\begin{cases} \dfrac{\mathrm{d}T_j}{\mathrm{d}t} = \displaystyle\sum_{i=1}^{N_j} S_{ij}(\theta, T_j) \\ T_j(0) = T_\infty. \end{cases} \tag{11}$$

In Figure 2, we have at a given time t_n, a schematic representation of the fire contour predicted by the model and the real fire contour. In the model, the cells defined on the fire contour have a temperature $T_j(t_n)$ obtained from (10), different from the ignition temperature T_{ign}. For a good

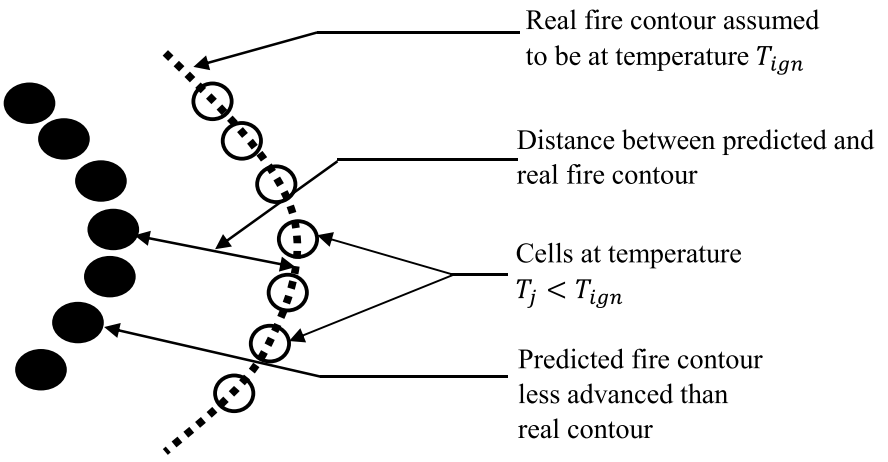

Figure 2. Schematic representation of the optimization method.

prediction, one should have $T_j(t_n) = T_{\text{ign}}$ at t_n. The aim of the method is to determine the vector $\theta \in \Omega$ which carries out at this instant, the predicted fire contour that matches the best to the experimental contour. That comes to determining for all the cells of the contour, the set of parameters that minimize the difference between two temperatures

$$\min_{\theta\in\Omega} \sum_{j=1}^{M_c} (T_j(\theta, t_n) - T_{\text{ign}})^2, \tag{12}$$

where M_c is the number of cells aligned on the real fire contour.

The temperature $T_j(\theta, t_n)$ is approximated by $T_j^{(n)}(\theta)$ obtained from (11) by solving the following fourth order Runge–Kutta scheme

$$\begin{cases} T_j^{(n-1,2)} = T_j^{(n-1)} + \dfrac{\Delta t}{2} \displaystyle\sum_{i=1}^{N_j} S_{ij}(\theta, T_j^{(n-1)}) \\ T_j^{(n-1,3)} = T_j^{(n-1)} + \dfrac{\Delta t}{2} \displaystyle\sum_{i=1}^{N_j} S_{ij}(\theta, T_j^{(n-1,2)}) \\ T_j^{(n-1,4)} = T_j^{(n-1)} + \Delta t \displaystyle\sum_{i=1}^{N_j} S_{ij}(\theta, T_j^{(n-1,3)}) \\ T_j^{(n)} = T_j^{(n-1)} + \dfrac{\Delta t}{6} \displaystyle\sum_{i=1}^{N_j} (S_{ij}(\theta, T_j^{(n-1)}) + 2S_{ij}(\theta, T_j^{(n-1,2)}) + 2S_{ij}(\theta, T_j^{(n-1,3)}) + S_{ij}(\theta, T_j^{(n-1,4)})). \end{cases} \tag{13}$$

In (13), $T_j^{(n-1)}$ is the approximation of the temperature of cell j at times t_{n-1} and Δt is the constant time step of discretization.

From (13), we can by induction express the temperature $T_j^{(n)}$ with respect to the initial temperature T_∞, that is,

$$T_j^{(n)} = T_\infty + \frac{\Delta t}{6} \sum_{l=1}^{n-1} \sum_{i=1}^{N_j} (S_{ij}(\theta, T_j^{(l)}) + 2S_{ij}(\theta, T_j^{(l,2)}) + 2S_{ij}(\theta, T_j^{(l,3)}) + S_{ij}(\theta, T_j^{(l,4)})). \tag{14}$$

Finally, the optimization problem is

$$\min_{\theta\in\Omega} \sum_{j=1}^{M_c} \left(T_\infty + \frac{\Delta t}{6} \sum_{l=1}^{n-1} \sum_{i=1}^{N_j} (S_{ij}(\theta, T_j^{(l)}) + 2S_{ij}(\theta, T_j^{(l,2)}) + 2S_{ij}(\theta, T_j^{(l,3)}) + S_{ij}(\theta, T_j^{(l,4)})) - T_{\text{ign}} \right)^2. \tag{15}$$

The resolution of (15) is performed using the Scilab-6.0.1 software [16].

Table 1. Model parameters used for F19 fire prediction

Parameters	Before calibration	After calibration
Fuel bed absorptivity a_{fb} (-)	0.6	0.998
Flame temperature T_{fl} (K)	1083	1106.66
Ember emissivity ε_b (-)	1	1
Fuel bed emissivity $\varepsilon_{\mathrm{fb}}$ (-)	0.6	0.1
Thermal conductivity of flame k_{fl} (W/mK)	0.0707	0.225
Thermal conductivity of ember k_b (W/mK)	0.0454	0.105
Ember temperature T_b (K)	561	561.41

4. Results

In this section, three experiments simulated by the optimized model are presented. The time is set at t_1, that is to say the calculations are limited to the first fire contour.

First, the model predictions of fire contours from two large-scale experimental fires are presented. These fire experiments were carried out in the savanna of the Northern Australia by N. Cheney *et al.* [17, 18]. The first experiment is called F19 and the second C064. These experiences have already been used in our previous work [11]. The fire F19 was incorrectly predicted by the initial model. Therefore, we reassess the prediction of this fire with the calibrated parameters.

Second, we also show the results of the laboratory-scale experiments that were used to test the initial model [11]. This is the experiences of D.R. Weise and G.S. Biging [19, 20]. The fuel characteristics and the test conditions of these wind tunnel experiments were well-controlled and well-documented.

These three experiments have been used to test several models in the literature [3, 4].

4.1. *Prediction of F19 fire experiment*

The optimization method described above is applied to F19 fire.

The fuel in F19 fire experiment is *Themeda* grass with a mean surface-area-to-volume ratio of 12,240 m^{-1} and a mean fuel load equal to 0.313 $\mathrm{kg/m}^2$. The size of the grassland plots is 200 m × 200 m and the ignition line fire is 175 m long and created in a duration of 56 s in opposite directions. The other input data are: wind speed $U_w = 4.8$ m/s, height of fuel bed $H = 0.51$ m, mass fraction of water $W = 0.058$, fuel particle density $\rho = 512$ $\mathrm{kg/m}^3$, specific heat capacity $C_p = 1480$ J/kgK, flame length $L_{\mathrm{fl}} = 2.7$ m, and ambient temperature $T_\infty = 307$ K. Fuel properties that are not provided by the authors are obtained from the literature.

The initial parameters of the model and the optimal parameters used to simulate F19 experiment are given in Table 1.

The predicted (bold lines) and real (symbol lines) contours are shown in Figure 3 at times 56 s, 86 s, and 138 s. On Figure 3(a) the prediction is made with the initial parameters, and on Figure 3(b) with the calibrated parameters. The predicted fire contour with the initial parameters is less advanced than the real contour at 56 s, 86 s, and 138 s (Figure 3(a)). The relative error on the rate of spread of the fire is 25%.

The predicted contour with optimal parameters and the real contour are in relatively good agreement at 56 s and 86 s (Figure 3(b)). The relative error made on the rate of spread is 8%. Prediction is therefore better at the optimal parameters.

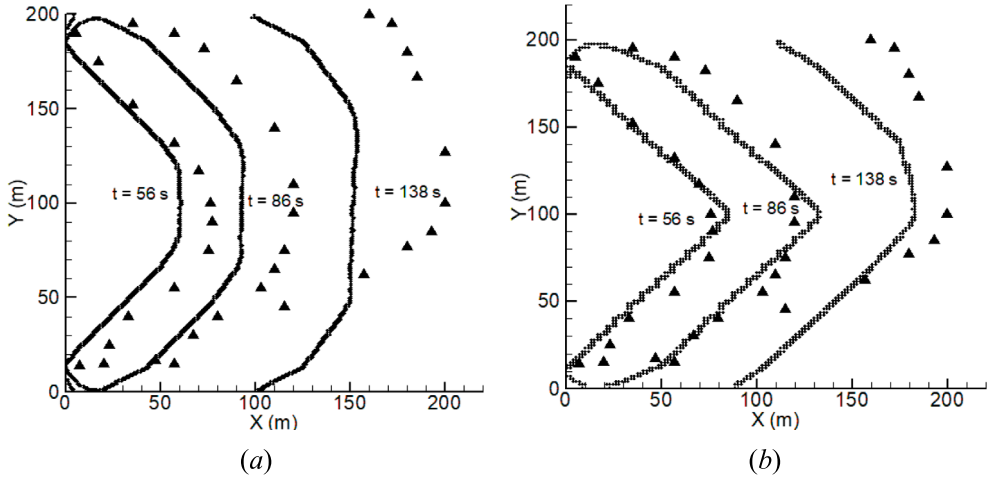

Figure 3. Comparison between predicted (bold lines) and real (symbol lines) fire contours: (a) prediction with initial parameters; (b) prediction with calibrated parameters.

Table 2. Model parameters used for C064 fire prediction

Parameters	Before calibration	After calibration
Fuel bed absorptivity a_{fb} (-)	0.6	0.69
Flame temperature T_{fl} (K)	1083	1083
Ember emissivity ε_b (-)	1	1
Fuel bed emissivity $\varepsilon_{\mathrm{fb}}$ (-)	0.6	1
Thermal conductivity of flame k_{fl} (W/mK)	0.0707	0.0371
Thermal conductivity of ember k_b (W/mK)	0.0454	0.0205
Ember temperature T_b (K)	561	561

4.2. *C064 fire prediction*

In this section, the results of the simulation of the C064 experiment with the optimized model are presented. The fuel in C064 fire experiment is *Eriachne* grass with a mean surface-area-to-volume ratio of 9770 m^{-1} and a mean fuel load equal to 0.283 $\mathrm{kg/m}^2$. The size of the grassland plots is 104 m × 108 m and the ignition line fire is 50 m long and created in a duration of 26 s in opposite directions. The other input data are: wind speed $U_w = 4.6$ m/s, height of fuel bed $H = 0.21$ m, mass fraction of water $W = 0.063$, fuel particle density $\rho = 512$ $\mathrm{kg/m}^3$, flame length $L_{\mathrm{fl}} = 4$ m, and ambient temperature $T_\infty = 305$ K.

Figure 4 presents the comparison of the predicted contours before and after calibration of the parameters with the real fire contours. The results predicted with the initial parameters are in good agreement with the experimental results (Figure 4(a)). These results are practically the same with the optimized model (Figure 4(b)). The initial and the optimal parameters used to simulate C064 experiment are given in Table 2.

At 100 s, the model overpredicts the spread rate of the flank fires in both cases. The propagation mechanism in a flank fire is complex and is the subject of research within the scientific community [3].

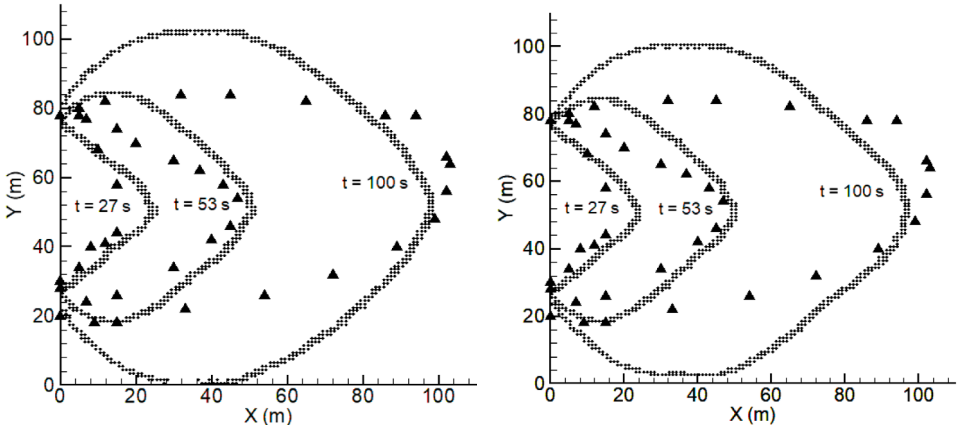

Figure 4. Prediction of the C064 experiment with (a) initial parameters; (b) optimal parameters. Bold lines are predicted fire contours and symbol lines are real fire contours.

Table 3. Model input data used for Laboratory-scale fire prediction

Experiment	Weise (white birch)
Flame length (m)	0.08–1.69
Ambient wind speed (m/s)	0–1.15
Fuel bed slope (°)	−15–+15
Initial water mass fraction (-)	0.11
Fuel bed thickness (m)	0.114
Ambient temperature (K)	303
Flame temperature (K)	1083
Ignition temperature (K)	500
Fuel density (kg/m^3)	609
Surface-to-volume ratio of fuel particles (m^{-1})	17.5
Fuel bed absorptivity (-)	0.6
Fuel bed emissivity (-)	0.9

4.3. *Laboratory-scale experimental data*

Weise's experimental data for flame propagation on very porous white birch fuel beds in a laboratory wind tunnel are compared to this model. The purpose of these experiments was to examine wind and slope interaction effects on flame properties. A tilting wind tunnel with an adjustable roof and 2.5 m long by 0.9 m wide test section was used. The data used for the simulations are summarized in Table 3.

In Figure 5, the predicted flame spreads are depicted according to the experimental flame spreads. The circular symbols are the flame spreads predicted with the calibrated parameters. The distance to the linear line, measures the error of the model. As can be seen in the figure, all of the symbols in circle are on this line unlike the others symbols. So, we have a better prediction with the calibrated parameters.

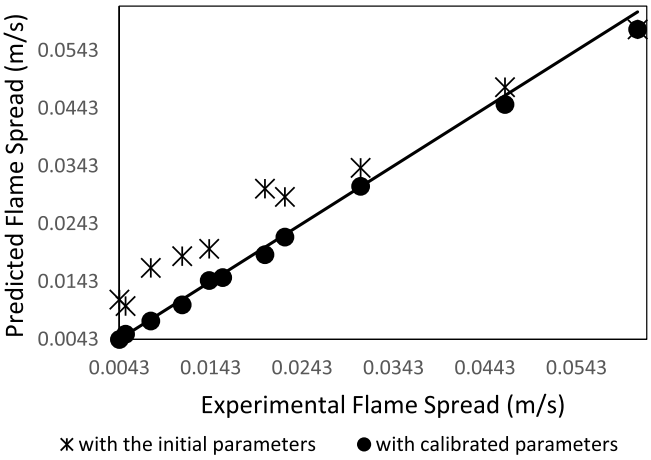

Figure 5. Comparison of predicted and real flame spread. Circular symbols are prediction with optimal parameters and the other symbols are prediction with initial parameters.

5. Conclusion

A mathematical optimization method was applied to the parametric model of fire propagation. The optimization problem is obtained after a formulation adapted to the propagation model. The seven parameters linked to the model have been optimized.

The prediction of the optimized model was tested on laboratory experiments and two large-scale experimental fires. Good agreement has been shown with the experimental data.

Even if the tests presented have confirmed the quality of the proposed method, additional large-scale experiments are necessary to evaluate and validate the model.

References

[1] B. Porterie, D. Morvan, J. C. Loraud, M. Larini, "Firespread through fuel beds: Modeling of wind-aided fires and induced hydrodynamics", *Phys. Fluids* **12** (2000), p. 1762-1782.

[2] R. R. Linn, P. Cunningham, "Numerical simulations of grass fires using a coupled atmosphere-fire model: Basic fire behavior and dependence on wind speed", *J. Geophys. Res.* **110** (2005), article no. D13107.

[3] W. Mell, M. A. Jenkins, J. Gould, P. Cheney, "A physics-based approach to modelling grassland fires", *Int. J. Wildland Fire* **16** (2007), p. 1-22.

[4] E. Koo, P. Pagni, S. Stephens, J. Huff, J. Woycheese, D. Weise, "A simple physical model for forest fire spread rate", *Fire Saf Sci.* **8** (2005), p. 851-862.

[5] S. Yassemi, S. Dragićević, M. Schmidt, "Design and implementation of an integrated GIS-based cellular automata model to characterize forest fire behaviour", *Ecol. Model.* **210** (2008), p. 71-84.

[6] J. K. Adou, Y. Billaud, D. A. Brou, J.-P. Clerc, J.-L. Consalvi, A. Fuentes, A. Kaiss, F. Nmira, B. Porterie, L. Zekri, N. Zekri, "Simulating wildfire patterns using a small-world network model", *Ecol Model.* **221** (2010), p. 1463-1471.

[7] P.-A. Santoni, J.-B. Filippi, J.-H. Balbi, F. Bosseur, "Wildland fire behaviour case studies and fuel models for landscape-scale fire modeling", *J. Combust.* **2011** (2011), p. 1-12.

[8] A. S. Bova, W. E. Mell, C. M. Hoffman, "A comparison of level set and marker methods for the simulation of wildland fire front propagation", *Int. J. Wildland Fire* **25** (2016), p. 229-241.

[9] D. Ascoli, B. Giovanni, V. Giorgio, "Calibrating Rothermel's fuel models by genetic algorithms", *Adv. Forest Fire Res.* (2014), p. 102-106, doi:10.14195/978-989-26-0884-6_10.

[10] T. Artés, A. Cencerrado, A. Cortés, T. Margalef, "Time aware genetic algorithm for forest fire propagation prediction: exploiting multi-core platforms: Time aware genetic algorithm for forest fire propagation prediction: exploiting multi-core platforms", *Concurr. Comput. Pract. Exp.* **29** (2017), article no. e3837.

[11] J. K. Adou, A. D. V. Brou, B. Porterie, "Modeling wildland fire propagation using a semi-physical network model", *Case Stud. Fire Saf.* **4** (2015), p. 11-18.

[12] F. M. White, *Heat Transfer*, Addison-Wesley, Reading, MA, 1984.
[13] K. M. Bryden, K. W. Ragland, C. J. Rutland, "Modeling thermally thick pyrolysis of wood", *Biomass Bioenergy* **22** (2002), p. 41-53.
[14] B. V. Babu, A. S. Chaurasia, "Heat transfer and kinetics in the pyrolysis of shrinking biomass particle", *Chem. Eng. Sci.* **59** (2004), p. 1999-2012.
[15] K. Zeng, J. Soria, D. Gauthier, G. Mazza, G. Flamant, "Modeling of beech wood pellet pyrolysis under concentrated solar radiation", *Renew. Energy* **99** (2016), p. 721-729.
[16] Scilab Company, "Scilab", 2019, http://www.scilab.org.
[17] N. Cheney, J. Gould, W. Catchpole, "The influence of fuel, weather and fire shape variables on fire-spread in grasslands", *Int. J. Wildland Fire* **3** (1993), p. 31-44.
[18] N. Cheney, J. Gould, W. Catchpole, "Prediction of fire spread in grasslands", *Int. J. Wildland Fire* **8** (1998), p. 1-13.
[19] D. R. Weise, G. S. Biging, "A qualitative comparison of fire spread models incorporating wind and slope effects", *For. Sci.* **43** (1997), p. 170-180.
[20] D. R. Weise, G. S. Biging, "Effects of wind velocity and slope on fire behavior", *Fire Saf. Sci. - Proc. Fourth Int. Symp.* **4** (1994), p. 1041-1051.